BioNanoScience (2024) 14:2854–2871
https://doi.org/10.1007/s12668-024-01353-9

RESEARCH

Characterization and Comparative Investigation of In Vitro Bioactivities for *Lactuca anatolica* Root Aqueous Extract and Their Green-Chemical Synthesized Nanoparticles; Molecular Docking Studies

Noor Nayel[1] · Sarmad Marah[1] · Tevfik Ozen[1] · Ilyas Yıldız[2,3] · Ramazan Erenler[2,4] · Lutfi Behcet[5]

Accepted: 29 February 2024 / Published online: 25 May 2024
© The Author(s), under exclusive licence to Springer Science+Business Media, LLC, part of Springer Nature 2024

Abstract

The current study synthesized silver nanoparticle (AgNP) biosynthesis and sustainable biochemical approaches, molecular docking studies using endemic and medicinal *L. anatolica* root aqueous extract. AgNPs were characterized in detail by TEM, XRD, and spectroscopic techniques such as FT-IR and UV–vis. The bioactivity of AgNPs was investigated with antioxidant, anti-inflammatory, photocatalytic, antibacterial, enzyme inhibition, and DNA protection tests. The AgNP formation was verified by UV–vis examination at 440 nm and the XRD, which showed a clearly defined crystalline organization. The TEM picture revealed uniformly distributed with a spherical shape and an average diameter of 17.5 nm. The synthesized AgNP exhibited PMRA ($A_{0.5}$, 0.10 µg/mL), RPA ($A_{0.5}$, 1.17 µg/mL), LPI (IC_{50}, 1.10 µg/mL), $DPPH^{\bullet}$ (IC_{50}, 2.61 µg/mL), and $ABTS^{\bullet+}$ (IC_{50}-6.21µg/mL) scavenging activities higher activity than the aqueous extract and the standards. Photocatalytic activity of AgNP exhibited significant methylene blue dye degradation efficiency when exposed to visible light for 5 h. AgNP displayed efficient inhibition of BSA denaturation with 57.58% at 125 µg/mL. Urease, BChE, and α-amylase inhibition activities of AgNP were more effective than aqueous extract and drugs. AgNP had excellent antibacterial activities, with an 8.5 and 9.0 mm inhibition zone against *Bacillus cereus* and *Enterococcus faecalis*. In silico studies chlorogenic acid-AgNP interaction product, the antibacterial activity of AgNPs was consistent with their in vitro effectiveness, as high molecular docking scores between − 203 and − 238. It was observed that AgNP protected DNA against oxidative damage more than quercetin. This is the first report confirming the strong antioxidation, antimicrobial, enzyme regulatory, anti-inflammatory, photocatalytic, and DNA protector of aqueous extract and AgNP.

Keywords *Lactuca anatolica* L. root · Aqueous extract · AgNP · Bioactivity · Molecular docking

✉ Tevfik Ozen
tevfikoz@omu.edu.tr

Noor Nayel
noorthu19@gmail.com

Sarmad Marah
sarmad159159@gmail.com

Ilyas Yıldız
ilyas.yildiz@igdir.edu.tr

Ramazan Erenler
rerenler@gmail.com

Lutfi Behcet
lbehcet@bingol.edu.tr

[1] Department of Chemistry, Faculty of Science, Ondokuz Mayıs University, 55139 Samsun, Türkiye

[2] Research Laboratory Practice and Research Center, Igdir University, 76000 Igdir, Türkiye

[3] Department of Nutrition and Dietetics, Faculty of Health Sciences, Igdir University, Igdir, Türkiye

[4] Department of Chemistry, Faculty of Arts and Sciences, Tokat Gaziosmanpasa University, 60240 Tokat, Türkiye

[5] Department of Molecular Biology and Genetics, Faculty of Arts and Sciences, Bingol University, 12000, Bingol, Türkiye

1 Introduction

In addition to their exceptional optical, electrical, and antibacterial capabilities, metal nanoparticles like Ag have attracted much attention over the years. However, these nanoparticles' poisonous properties and aggregation have restricted their usage in more effective applications [1, 2]. The surface of these particles can be functionalized with therapeutically effective biomolecules, which will undoubtedly improve their biocompatibility and biological application [3]. Nano Ag is not a new concept. Lea published the first synthesis of an Ag colloid stabilized by citrate in 1889. Though not technically recognized or known as "nano," literature suggests that Ag colloids have been utilized in the medical field under the term "Collargol" for more than 100 years, dating back to 1897. In the USA, the earliest biocidal Ag substance "Algaedyn" was registered in 1954, and it is being used in disinfectants today. The progress of nanotechnology over the last two decades has opened up new opportunities for AgNPs. Because AgNPs are at the nano-scale dimension, they have several novel characteristics compared to the bulk metal, which has sparked considerable interest in creating new usage [4].

Creating eco-friendly techniques that do not employ hazardous chemicals in the synthesis protocols is becoming increasingly critical in the modern world. Green synthesis techniques have benefits over traditional procedures that use chemical agents linked to environmental damage [5]. These techniques include mixed-valence polyoxometalates, polysaccharides, Tollens, and biological and irradiation processes [6]. Regarding the green synthesis of nanoparticles, the most crucial factors to consider are the choice of solvent medium and the choice of non-toxic, environmentally friendly reducing and stabilizing agents [7]. Given this, the present investigation aimed to evaluate the biological efficacy of Ag nanoparticles synthesized from *Lactuca anatolica* root extract.

The Asteraceae, or Compositae family, is one of the most well-known plant families. Except for Antarctica, this plant family has colonized every continent and thrived in various settings [8]. The Asteraceae family has around 1600 genera and 23,000 species [9–11]. Many Asteraceae plants have medicinal properties. According to chemo-taxonomic features, the most significant main chemical group in this family is flavonoids, coumarins, diterpenes, polyacetylenes, oxygenated sesquiterpenes, and sesquiterpene lactones, which are responsible for the plant's therapeutic effects [12, 13]. Although many Asteraceae species contain antimicrobial and protective chemicals, the biological activities of such plants are still not substantially explored. Many Asteraceae plants are currently treasured for their applications in the kitchen and the medicinal profession. They do well in semiarid and subtropical settings. Multiple species of the Compositae family have been used for health purposes, including those with antibacterial and anti-inflammatory properties [14].

Lactuca types like *L. sativa* and *L. ulva* allow long-term particle production [15–17]. The investigation revealed the antibacterial efficacy of nanoparticles against *B. subtilis*, *S. aureus*, *K. pneumonia*, and *E. faecalis*. *L. ulva* also possesses substantial reduction and DPPH$^{\bullet}$ scavenger abilities. Applying marine green macro-algal *L. ulva* extract, a group of academics developed nanoparticles that targeted the HCT-116 cell line and were active against malignant cells. According to the findings, *L. ulva* nanoparticles might be effective in targeted anticancer therapies [18, 19].

According to the relative scarcity of scientific study on *L. anatolica* (Asteraceae: *Lactucinae*), a taxonomically distinctive member of the acclaimed botanical lineage under consideration, [20] its potential medicinal benefits must be investigated. Considering the immense medicinal importance of *Lactuca* species, the *L. anatolica* root aqueous extract and the synthesized AgNP were conducted to develop a sustainable approach and evaluate a therapeutic potential. The different in vitro effects of AgNP synthesized from *L. Anatolica* root aqueous extract, which is also used by the public for different purposes, have not been investigated in previous publications. Therefore, the in vitro antioxidant, enzyme inhibition, antibacterial, anti-inflammatory, and DNA protection properties of the aqueous extract and biosynthesized AgNPs need to be investigated and examined in detail. In addition, the antibacterial effects of the recommended AgNP product, based on the main component of the aqueous extract, were examined through molecular docking studies.

The different in vitro effects of AgNP synthesized from *L. Anatolica* root aqueous extract have not been investigated in previous publications. Therefore, the in vitro antioxidant, enzyme inhibition, antibacterial, anti-inflammatory, and DNA protection properties of the aqueous extract and biosynthesized AgNPs need to be investigated and examined in detail. In addition, the antibacterial effects of the recommended AgNP product, based on the main component of the aqueous extract, were examined through molecular docking studies. HPLC–MS/MS analysis of the aqueous root extract in which AgNP was biosynthesized was performed. Additionally, molecular docking was applied to the interactions between the main component-NP and antibacterial targets for antibacterial testing. Biosynthesized AgNP was characterized by ultraviolet–visible (UV–vis), Fourier transform infrared spectroscopy (FTIR), scanning electron microscopy (SEM), X-ray diffraction (XRD), and transmission electron microscopic (TEM). Antioxidation activity was tested by determining phosphomolybdate reducing assay (PMRA),

reducing power assay (RPA), lipid peroxidation inhibition (LPI), free radical (DPPH˙), and $ABTS^{\bullet+}$ scavenging effects. Enzyme inhibition capacity was determined with α-amylase, urease, acetylcholinesterase (AChE), and butyrylcholinesterase (BChE) enzymes. Disc diffusion and microdilution methods were used for antimicrobial activity. Additionally, anti-inflammatory, photocatalytic, and DNA protection activities were applied with molecular docking. This work aims to provide a fresh prespective on the bioactivity testing and of AgNPs by using spectroscopic analysis, bioactivity tests, and molecular docking investigations to root water extract and biosynthesized AgNP for the first time.

2 Materials and Methods

2.1 Plant Collection

Roots of *L. anatolica* (Asteraceae: *Lactucinae*) were procured from Bingol, Turkey. The *L. anatolica* roots (LAR) were gathered by Prof. Dr. Lutfi Bechet, instructor in the Biology Department, Faculty of Sciences and Arts, Bingöl University. A voucher specimen was submitted to the herbarium with voucher number BIN17939.

2.2 Extract Preparation

Fresh roots (R) were removed from whole plants and cleaned in tap water to remove soil particles. They were dried in airflow at room temperature. Dry root samples were entirely pulverized by electric crushing. One hundred milliliters of distilled water and root powder (40 g) were mixed homogeneously and incubated in a water bath. The aqueous (AQ) extract was filtered through Whatman no. 1 filter paper, lyophilized, and dried. The crude LAR-AQ extract was stored at − 20 °C.

2.3 Ag nanoparticle (AgNP) Synthesis

For Ag nanoparticle (AgNP) biosynthesis, 100 mL of 0.071 mM $AgNO_3$ aqueous solution was added to 25 mL of freshly prepared LAR-AQ extract [21]. The reaction mixture was stirred continuously at pH 7 and 65 °C for 2 h. At the end of the reaction, the color transformation showing the synthesis of AgNP, which consists of the reduction reaction of $Ag^{+}_{(aq)}$ ions to $Ag^{0}_{(aq)}$, was observed and analyzed.

2.4 Characterization Processes of AgNPs

For the characterization of LAR-AgNP, AgNP prepared under optimized conditions was centrifuged at 10,000 × g for 25 min at 4 °C [21]. The resulting residue was wholly dried in the lyophilizer. Using UV–vis spectrophotometry (UV–vis, UV-2600), the spectral analysis of *L. anatolica* root Ag nanoparticle (LAR-AgNP) was ascertained in the range of 300–700 nm to scan the reduction of $AgNO_3$. Fourier transform infrared spectroscopy (FTIR) analysis was evaluated in ATR mode (FT/IR-4000, ATR-Pro One, FTIR 4700, JASCO) to identify the chemical groupings of natural compounds that were serving as reducing, capping, and stabilizing agents involving in the bio-reduction of $AgNO_3$. Transmission electron microscopic (TEM) with EDX (Quanta Feg450) analyses were used to visualize the morphology and particle diameter of the nanoparticles. The crystal structure of AgNPs was examined using X-ray diffraction (XRD, Empyrean, Malvern Panalytical Diffractometer) [22].

2.5 Quantification of Total Phenolic and Flavonoid

Total phenolic content (TPC) and total flavonoid content (TFC) of LAR-AQ extract were determined by Singleton and Rossi [23] and Chang, Yang, Wen, and Chern [24] using the methods applied, respectively. TPC and TFC values of samples mg gallic acid as equivalent (GAE) and mg quercetin expressed as equivalents (QE), respectively.

2.6 HPLC–MS/MS Analysis

The LAR-AQ extract (50 mg) was put into tube to conduct with LC–MS/MS analysis. After adding 2 mL of ethanol, the mixture was swirled. Hexane was used to remove the generated mixture. The final combination was centrifuged and agitated for 10 min at 9000 rpm. From the resultant solution, 100 µL of the methanol phases were sampled, and the volume was diluted to 900 µL using a ratio of 450 (water)/450 (methanol). The final sample was filtered and subjected to LC/MS–MS analysis at a temperature of 40 °C, a 5.12 mL injection volume, a 0.4 mL/min flow rate, and a 30-min procedure time.

2.7 Antioxidant Activity

The antioxidant activity was performed with IC_{50}, and $A_{0.5}$ values were predicted based on the activity results. At the effective concentration of 0.5 absorbances, phosphomolybdate reducing assay (PMRA) and reducing power assay (RPA) were found to be $A_{0.5}$ (µg/mL). For lipid peroxidation inhibition (LPI), free radical (DPPH˙), and $ABTS^{\bullet+}$ scavenging activities, IC_{50} values (µg/mL) are also presented as half-maximal capture concentrations of 50% [25]. The antioxidant activities of LAR-AQ extract and LAR-AgNP were determined at 695 nm for PMRA [26], at 700 nm for RPA [27], at 517 nm for DPPH˙ scavenging activity [28], at 734 nm for $ABTS^{\bullet+}$ radical scavenging activity [29], and at 532 nm for LPI activity [30]. Ascorbic acid, trolox, and BHT were tested with extract and compared with standard compounds.

2.8 Enzyme Inhibitory Activity

α-Amylase [31], urease [32], acetylcholinesterase (AChE), and butyrylcholinesterase (BChE) [33, 34] inhibitory activities of LAR-AQ extract and LAR-AgNP were studied. In these assays, applying a reader for microplates, the samples' ability to inhibit enzymes was evaluated, and the sample concentration needed to achieve a 50% reduction in maximal activity was computed. For any enzyme inhibiting test, including, the half-inhibitory concentrations (IC_{50}) of LAR-AQ extract and LAR-AgNP were assessed. Standard medications were also contrasted.

2.9 Antibacterial Activity

To evaluate the inhibition zone (IZ) and minimal inhibitory concentration (MIC) of the LAR-AQ extract and optimized LAR-AgNP against tested six bacterial strains, we tested the disc diffusion and microdilution methods, as previously reported [35]. The bacterial strains were cultured on Mueller–Hinton agar (MHA, 38 g/L ddH_2O) medium and were kept at 37 °C for 24 h in a sterile cabinet. Three of the bacteria were gram-negative (*Pseudomonas aeruginosa*, ATCC 15442; *Escherichia coli*, ATCC 25922; *Klebsiella pneumonia*, ATCC 10031), and three of the bacteria were gram-positive (*Bacillus cereus*, CCM 99; *Enterococcus faecalis*, ATCC 29212; and *Staphylococcus aureus*, ATCC 25213). The *B. cereus* strain was incubated for 16 to 18 h at 30 °C. Before beginning the activity, every culture of bacteria needed to be diluted to the McFarland turbidity standard of 0.5 (1.5×10^8 CFU/mL) and homogenized using sterile saline (0.85% NaCl) mixture.

Using the disc diffusion technique, the samples' antibacterial activity was ascertained [36]. The sterilized Petri dishes were filled with 25 mL of Mueller–Hinton agar (MHA). After adding a few bacteria, 5 mL of sterile saline (0.85% NaCl) solution was added, and the McFarland adjustment was set to 0.5. The sample (50 µL) was absorbed into discs before being put on agar, and the bacterial solution with the McFarland value adjusted to 0.5 was added to the agar. It was incubated for 16 to 18 h at 37 °C. The inhibitory zone is given in millimeters. As positive controls, tetracycline and amoxicillin were administered.

Tests using extract and NP doses in a cationic Mueller–Hinton broth (MHB) medium were used to calculate the MIC. The findings were expressed in µg/mL. $MgCl_2$ and $CaCl_2$ were added at 2 mg/mL values to create the cationic MHB. The sterilized 96-well plate had 100 µL of extracts or antibiotics in each well. Five microliters of this product were added to each well after 1 mL of the bacterial solution containing 0.5 McFarland was combined with 9 mL of MHB. The plate was then incubated for 2 h at a temperature of + 4 °C. The procedure of incubation lasted exactly 18 h at 37 °C. Over 16–18 h, only *B. cereus* was maintained at 30 °C. Following that, the data were recorded, and the agar plates were visually examined for any indications of turbidity or growth.

2.9.1 Anti-inflammatory Activity

Research was conducted on the impact of LAR-AQ and LAR-AgNP on the denaturation of bovine serum albumin (BSA) protein in a somewhat different manner than Rahman, Eswaraiah, Vakati, and Madhavi [37]. Five hundred milligrams of 0.5% bovine serum albumin (BSA) were dissolved in 100 mL of water. Buffer of saline phosphate, pH 6.3: 8 g of sodium chloride (NaCl), 0.2 g of KCl, 1.44 g of Na_2HPO_4, and 0.24 g of KH_2PO_4 should all dissolve in 800 mL of pure water. The volume was raised to 1000 mL with distilled water, and the pH was adjusted to 6.3 using 1N HCl. The test solution (0.5 mL) comprises 0.45 mL of BSA (0.5% w/v aqueous solution) and 0.05 mL of the test solution at different concentrations. The test control solution (0.5 mL) consists of 0.05 mL of distilled water and 0.45 mL of BSA (0.5% w/v aqueous solution). A mixture of 0.05 mL test solution and 0.45 mL clean water makes up the product control (0.5 mL). 0.45 mL of BSA (0.5% w/v aqueous solution) and 0.05 mL of various dosages of diclofenac sodium are included in the standard solution (0.5 mL). The sample and diclofenac sodium solutions of 0.45 mL (0.5% w/v BSA) were mixed with 0.05 mL of various test medication concentrations (50, 100, and 250 µg/mL). The samples were incubated for 20 min at 37 °C and then for 3 min at 57 °C. After the solutions as mentioned above have cooled, add 2.5 mL of phosphate buffer. The absorbance was measured using a UV–vis spectrophotometer that was calibrated to 255 nm. The control shows the total denaturation of the protein. The results were contrasted with sodium diclofenac. The following formula may be used to get the % inhibition of protein denaturation.

$$\% \text{ Inhibition} = 100 - \frac{OD_{test} - OD_{control}}{OD_{test}} \times 100$$

2.9.2 Photocatalytic Activity

In this study, methyl blue (MB) was reduced and degraded to determine the catalytic activity of LAR-AQ extract and LAR-AgNP. The photocatalytic activity was measured in visible light using MB. Ten milligrams of LAR-AQ extract and LAR-AgNP were combined with aqueous MB solution (10 mg/L) to form a suspension. The mixture was then shaken in the dark for 30 min to test the samples' ability to

catalyze reactions. After that, the mixture was exposed to visible light for 4 h. The suspension was extracted in 3 mL at different intervals and centrifuged for 5 min at 4000 rpm. A UV–vis spectrophotometer was employed to examine the solution of the supernatant. The control was an MB solution (10 mg/L) without samples [38].

2.9.3 DNA Protection Activity

The DNA-protecting activities of LAR-AQ extract and LAR-AgNP were evaluated using agarose gel electrophoresis [39]. Two microliters of ethidium bromide were added to a 1% agarose gel after it had been created. After being placed inside the container, the agarose gel solidified for at least 2 h. The electrophoresis tank was then filled with the thicker gel. One time, the TBE buffer was added to the electrophoresis tank.

Negative control: DNA plasmid (3 µL)-ddH_2O (6 µL)-glycerol (4 µL).

Positive control: 3 µL of plasmid DNA-ddH_2O (6 µL)-glycerol (4 µL)-H_2O_2 (1 µL)-UV for 5 min.

The mixture of the sample: 3 µL of plasmid DNA-sample (5 µL)-glycerol (4 µL)-H_2O_2 (1 µL)-UV for a 5 min.

Two microliters of loading dye were applied to the control and sample. Wells were filled with 1000 µg/mL of sample and control and ran for 60 min at 90 V. Imaging was done using a UV transilluminator (320 nm, 8000 µW/cm).

2.9.4 Molecular Docking

In this research, we investigate the ability of novel Ag nanoparticles to explain their remarkable effect against different bacteria strains, using several antibacterial targets that have been widely used in the literature as antibiotic targets. Using the ChemDraw 18.0 Ultra program, we created the estimated structure of the Ag nanoparticles with the abundant compound in our aqueous extract (Chlorogenic acid-AgNP). After that, we reduced the total energy of the compound using the energy-minimizing tool of the Chem3D 18.0 program. After that, we obtained the complete structures of the antibiotic targets from the RCSB PDB with a suitable resolution: PDB ID:1AI9 for dihydrofolate reductase, PDB ID:3PTE for DD-peptidase, and PDB ID:2XCS for the gyrase [40]. Molecular docking was performed using the Molegro Virtual Docker (MVD) program to determine the interaction scores between the proteins and chlorogenic acid-AgNP [41, 42]. BIOVIA Discovery Studio Visualizer was applied to obtain the molecular docking product's 2D and 3D image shapes and identify the complete structure of antibacterial target proteins and our nanoparticles [43, 44].

2.9.5 Statistical Analysis

The biological activity's triple evaluations of each variable produced an average and a standard deviation. Using SPSS 20.0, the findings were statistically analyzed. If the data distribution was regular, the analytic mean would be considered homogeneous over more than two groups. It was utilized since Tukey's HSDa, b is a multiple comparison procedure. After comparing the values obtained from each activity analysis to the samples and standards, statistically significant differences ($p < 0.05$) occurred.

3 Results and Discussion

Various research studies have shown that medicinal, aromatic plants protect the human body against many damaging effects caused by oxidative stress. Medicinal plants contain a mixture of phytochemical compounds that can work alone or in combination to cure diseases and maintain health, as they are a good source of antioxidants [45]. Polyphenols are the major dietary phenolics, which include phenolic acids (hydroxybenzoic and hydroxycinnamic acids) and flavonoids. Flavonoids are the most comprehensively studied group of polyphenols [46]. The high phenolic content of plants has been associated with antioxidant activities analyzed by reducing power, lipid peroxidation inhibition, $DPPH^{\bullet}$, and $ABTS^{\bullet+}$ scavenging activities [45]. Antioxidant activity is also observed with the increase of specific compound contents such as gallic acid, chlorogenic acid, and cinnamic acid, which contain high amounts [47]. The total phenolic and flavonoid contents of LAR-AQ extract were 82.04 ± 1.10 mg GAE/g dry weight and 3.91 ± 2.29 mgQE/g dry weight, respectively. Harsha, Anilakumar, and Mithila [48] reported that the TPC and TFC of the hydro-alcohol extract of the leaf parts of the *L. sativa* plant were 158 µg GAE and 25.10 µg QE/g, respectively. Stojakowska and Malarz [49] determined that the TPC of the methanol extract of the *L. aculeata* plant was 39.79 ± 1.61 mg GAE/g. Gan and Azrina [50] found that five varieties of *L. sativa* were red coral in order of decreasing TPC: (76.05 mg GAE/100 g) > green coral (30.39 mg GAE/100 g) > romaine (9.14 mg GAE/100 g) > butter (4.92 mg GAE/100 g) > iceberg (4.85 mg GAE/100 g).

HPLC was employed for the quantitative measurement of *L. anatolica* root extract, and 40 standards were used (Fig. 1). Chlorogenic acid was identified as a significant product with a value of 0.58 mg/g extract. Caffeic acid (0.099 mg/g extract), trans-cinnamic acid (0.04 mg/g extract), and vanillin (0.007 mg/g extract) were also discovered in the extract (Table 1). Figure 2 shows the chemical structure of pharmaceutically relevant chemicals in LAR-AQ. The hydroxyl and carboxyl groups contained in phenolic compounds are

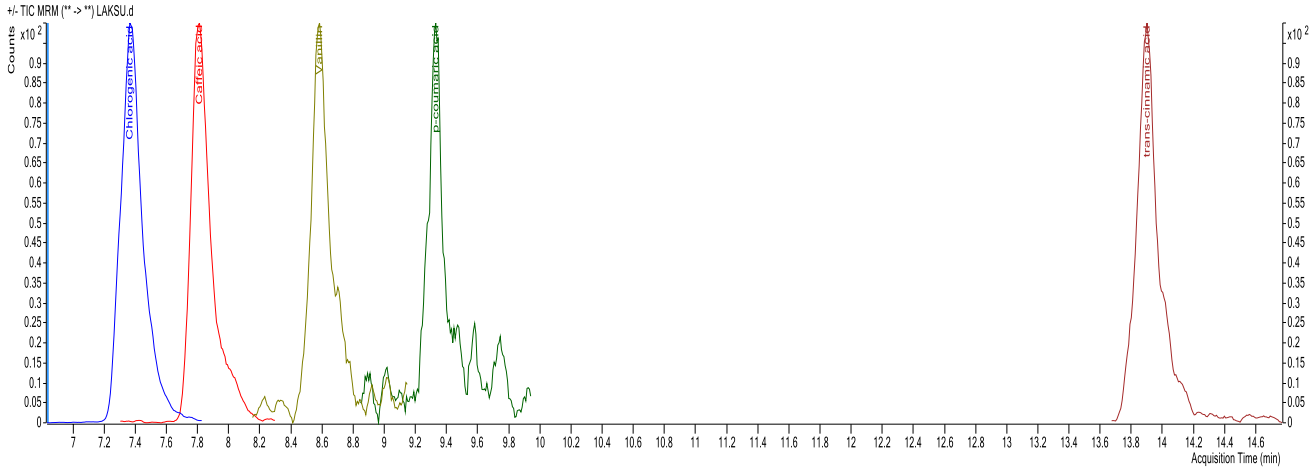


Fig. 1 HPLC–MS/MS chromatogram of LAR-AQ extract

more effective in interacting with Ag (Ag^+) ions and may be an active reducing power source in the formation of AgNPs [51]. Phenolic compounds cover the active surfaces of nanoparticles, providing further growth and stability of the structure in colloidal suspension [52].

3.1 Characterization of Green Synthesized AgNP

3.1.1 UV–vis Analysis of AgNP

LAR-AgNP synthesis was accomplished by transforming the aqueous ionic form $AgNO_3$ to solid metal nanoparticles. The color of the solution changed from green to black, indicating the formation of LAR-AgNP. However, UV–vis spectroscopy was utilized to examine these particles to give additional proof that the plant extract was employed to make nanoparticles. Figure 3 shows UV–vis spectra from aqueous root extracts containing NPs. Unlike the root extract, which showed no peaks, the AgNPs displayed a definite peak at 440 nm. Many researchers have applied the UV–vis spectra in order to track the synthesis of the nanoparticles, where in the Ag-NP UV–vis spectrum a notable peak is generally observed between 400 and 500 nm as in our findings [53].

3.1.2 FTIR Analysis of AgNP

The attenuated total reflectance (ATR) approach in Fourier transform infrared (FTIR) spectroscopy was utilized to ascertain the chemical makeup of AgNPs' active groups. Table 2 shows the related data, and Fig. 4 illustrates that the recorded spectra were acquired throughout the wavelength range of 400–4000 cm^{-1}. FT-IR bands at wave numbers 3182, 1569, 1373, 1234, and 1023 cm^{-1} were visible on the root. According to these findings, molecular functional groups may be responsible for reducing Ag ions, as seen in the pictures that go with this article. Aldehydes, alkanes, alcohols, and ether or epoxy groups are examples of phytochemical substances that may be present in biomass and are thought to be involved in the nucleation process that converts Ag + to Ag [54]. A variety of substances, including alkaloids, proteins, pigments, amides, amines, carbonyl groups, phenolics, flavonones, and terpenoids, as well as reduction factors found in biological extracts, can start the formation of nanoparticles [55].

3.1.3 TEM and XRD Analysis of AgNP

Ag nanoparticles on a carbon-coated copper transmission electron microscopic (TEM) grid produced the TEM image shown in Fig. 6. The micrograph presented here displays spherical AgNPs with a root size of 17.5 nm and a moderate density dispersion. The characterization of nanoparticles by TEM has been documented in a work by Sondi and Salopek-Sondi [56]. In our literature review, electron microscopy technique has been widely used in the characterization of nanoparticles, where this technique provides an important information about the synthesis of the particles and their stability in addition to their size and shape [57].

The clear peaks detected in the X-ray diffraction (XRD) scan provided additional proof and assurance that the synthesized AgNPs were correct (Fig. 5). The graph shows four peaks with relative values of 37.77, 44.15, 65.25, and 77.12, each corresponding to a distinct plane of Ag: 111, 200, 220, and 311. We found no contaminant peaks in the X-ray diffraction pattern. Because of the unique crystalline structure of the substance being investigated, X-rays are diffracted as they pass through it. This permits one to identify the crystalline structure of the material under investigation. Sambhy, MacBride, Peterson, and Sen [58] used this analytical

Table 1 Quantitation results of LAR-AQ extract by LC–MS/MS

No	Compound	R.T. (min^{-1})	Final conc. (mg/g)
1	Shikimic acid	1.38	*nd*
2	Gallic acid	3.83	*nd*
3	Protocatechuic acid	6.01	*nd*
4	Catechin	7.11	*nd*
5	Chlorogenic acid	7.37	0.5829
6	Hydroxybenzaldeyde	7.63	*nd*
7	Vanillic acid	8.19	*nd*
8	Caffeic acid	7.81	0.0989
9	Syringic acid	8.34	*nd*
10	Caffeine	8.39	*nd*
11	Vanillin	8.58	0.0072
12	*p*-Coumaric acid	9.33	*nd*
13	Salicylic acid	9.61	*nd*
14	Taxifolin	9.82	*nd*
15	Polydatin	9.74	*nd*
16	Resveratrol	9.73	*nd*
17	*Trans*-ferulic acid	10.14	*nd*
18	Sinapic acid	10.49	*nd*
19	Scutellarin	10.86	*nd*
20	Isoquercitrin	11.55	0.0040
21	o-Coumaric acid	11.40	*nd*
22	Coumarin	11.54	*nd*
23	Protocatehuic ethyl ester	11.79	*nd*
24	Rutin	11.81	*nd*
25	Hesperidin	11.51	*nd*
26	Quercetin-3-D-xyloside	12.65	*nd*
27	Kaempferol-3-glucoside	13.03	*nd*
28	Fisetin	13.32	*nd*
29	Baicalin	13.67	*nd*
30	Trans-cinnamic acid	13.90	0.0399
31	Quercetin	14.91	*nd*
32	Naringenin	14.94	*nd*
33	Hesperetin	15.85	*nd*
34	Morin	15.79	*nd*
35	Kaempferol	16.37	*nd*
36	Baicalein	17.03	*nd*
37	Luteolin	18.06	*nd*
38	Biochanin A	17.83	*nd*
39	Chrysin	17.87	*nd*
40	Diosgenin	23.45	*nd*

nd not detected

approach to assess the particle structure and confirm the existence of nanoparticles.

3.2 Antioxidant Activity

The PMRA activity was evaluated through the colorimetric application, which reduces the antioxidant's capacity to convert Mo^{+6} to phosphomolybdate Mo^{+5} complex. In this study, the PMRA capacity of AgNP was statistically more potent than that of the aqueous root extract, $p < 0.05$ (Table 3). The $A_{0.5}$ value of optimized AgNP was found to be more effective than trolox and ascorbic acid. The reason for the effective PMR activity of optimized and green synthesized AgNP can be attributed to the metal salt of LAR-AgNP in the phenolics and flavonoids of the aqueous extract. The LAR-AgNP, LAR-AQ, trolox, and ascorbic acid were shown in order by the PMRA.

The RPA activity was determined by spectroscopic monitoring. The LAR-AQ exhibited moderate activity in reducing Fe^{3+} ions, according to the observation of the $A_{0.5}$ value (Table 3). The creation of the Fe^{2+} extract complex caused a dependence upon concentration to rise in the absorbance of the *L. anatolica* extracts, indicating that the excerpts provided reactive free radicals with electron donations. The outcomes demonstrated that the LAR-AgNP extracts' reducing power outperformed ascorbic acids. The aqueous extracts of *L. anatolica* exhibited the following RPA capabilities ($Fe^{3+} \rightarrow Fe^{2+}$): LAR-AgNP > trolox > ascorbic acid > LAR-AQ. In Amin [59] investigation, the RPA values of *Ulva lactuca* aqueous extract and synthesized AgNP were 24.3 and 31.6 mg ascorbic acid/g, respectively, while the activity of AgNP synthesized from *L. anatolica* root aqueous extract was found to be more effective at 1.17 µg/mL.

$DPPH^{\bullet}$ is a free radical that transforms into a stable structure by accepting a single electron and is the most used molecule in antioxidant activity determinations. The transformation of the dark violet alcohol solution of $DPPH^{\bullet}$ into yellow hydrazine (DPPH-H) under the influence of an antioxidation indicates that it is reduced to $DPPH^{\bullet}$. The IC_{50} values for LAR-AQ extract, optimized LAR-AgNP, ascorbic acid, and trolox were 1.86 ± 0.34, 2.61 ± 0.66, $2.33 \pm 1.65.68$, and 1.36 ± 0.26 µg/mL, respectively (Table 3). González-Ballesteros, Rodríguez-Argüelles, Prado-López, Lastra, Grimaldi, Cavazza, Nasi, Salviati, and Bigi [60] determined the EC_{50} values of *Ulva lactuca* L. aqueous extract and synthesized AgNPs as 153.8 and 47.75 mg/mL, respectively, and our results were more effective radical scavenging activity. Similarly, Amin [59] reported the $DPPH^{\bullet}$ scavenging activity of AgNP synthesized from *Ulva lactuca* as 1.5 mg/mL.

Secondary metabolites have a more significant effect on the functioning of the antioxidation mechanism to eliminate proton radicals. The $ABTS^{\cdot+}$ scavenging activities of LAR-AQ extract and synthesized LAR-AgNP are in the order as follows: LAR-AgNP > trolox > ascorbic acid > LAR-AQ (Table 3). Although *L. anatolica* aqueous root extract did not effectively scavenge the cationic $ABTS^{\cdot+}$ radical, the synthesized AgNP was close to trolox and higher than ascorbic acid. Harsha, Anilakumar, and Mithila [48] reported the $ABTS^{\bullet+}$ scavenging activity of *L. sativa* ethanol extract as 472 µg/mL.

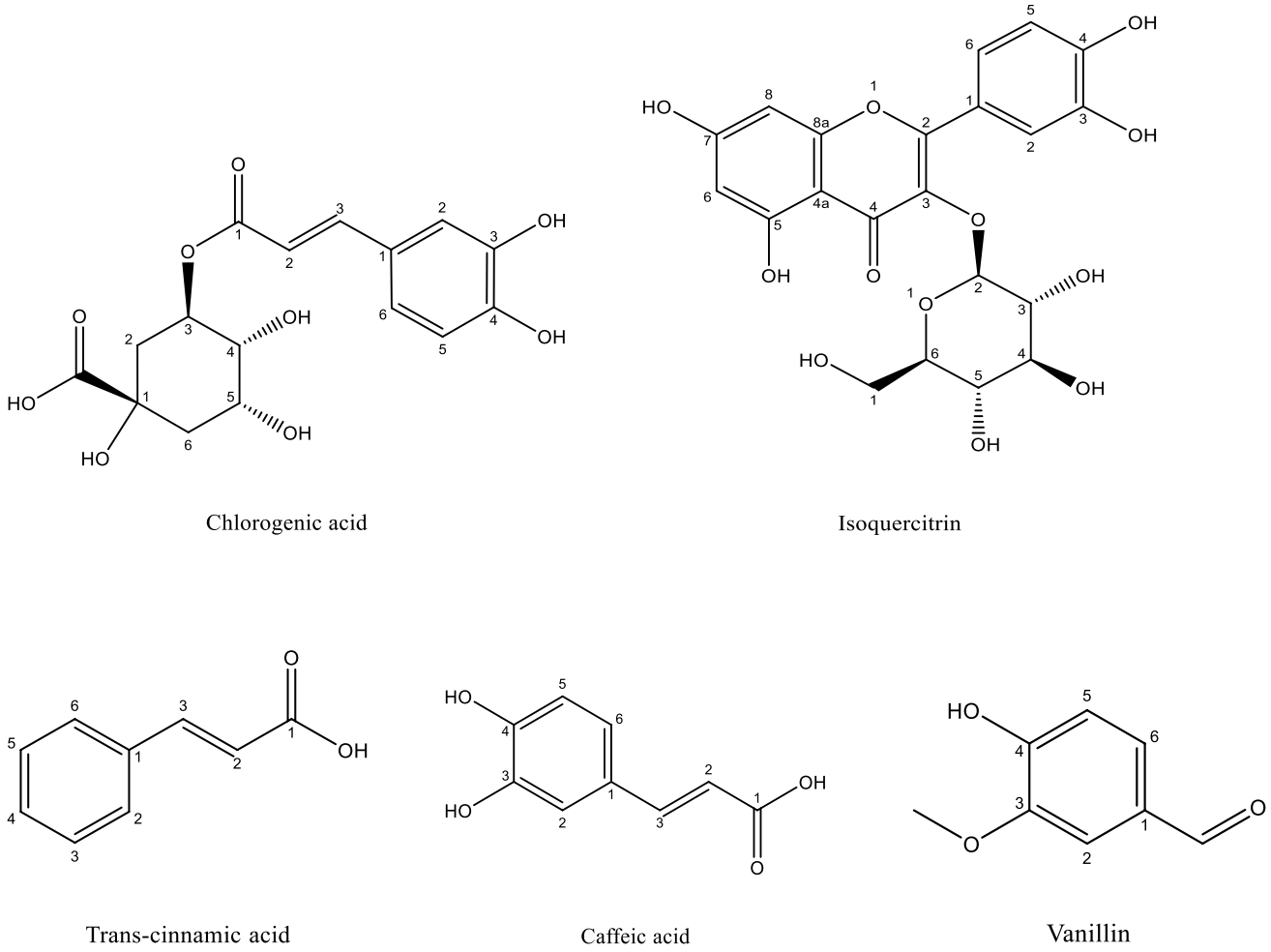


Fig. 2 The chemical structure of pharmaceutically significant compounds in LAR-AQ extract

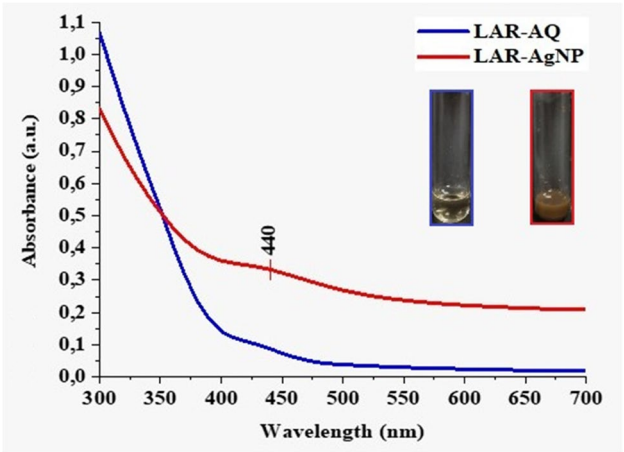


Fig. 3 UV–vis spectrums of LAR-AQ extract and synthesized LAR-AgNP

The extract's LPI activity decreased as follows: LAR-AgNP > LAR-AQ > ascorbic acid > trolox. LAR-AgNP extracts effectively inhibited LPI activity: their IC_{50} value was lower than that of ascorbic acid and trolox. Whether this nanoparticle is effective or not depends on the phenolic chemicals it contains. Linoleic acid was used, and the induction of lipid peroxides by Fe^{2+}/ascorbate-induced formation of thiobarbituric acid-reactive substances (TBARS) and by the loss of the polyunsaturated fatty acyl chains. The amount of lipid peroxidation and malondialdehyde (MDA) induced by reactive oxygen species (ROS) were determined using linoleic acid. AgNP was more effective than LAR-AQ extract in removing ROS that cause LPI (Table 3). This result may indicate that AgNP may be an effective product in protecting against peroxidation, cancer, membrane damage, and other diseases.

3.3 Enzyme Inhibitory

L. anatolica root extract and its optimized AgNP were investigated in vitro for their potential as inhibitors of urease, AChE, BChE, and α-amylase enzymes. Their effective results

Table 2 FT-IR data of LAR-AgNP

Wave number (cm^{-1})	Ligament/stretching	Functional groups
3720	O–H and N–H	Alcohols-phenols and amides
3127	C–H	Alcohols and amides
1915	C=O	Carbonyl compounds containing N–O bond (amides) and aldehydes, ketones and carboxylic acid
1099	C–O and C–N	C–O stretching
851	Ar–H	C-H bending

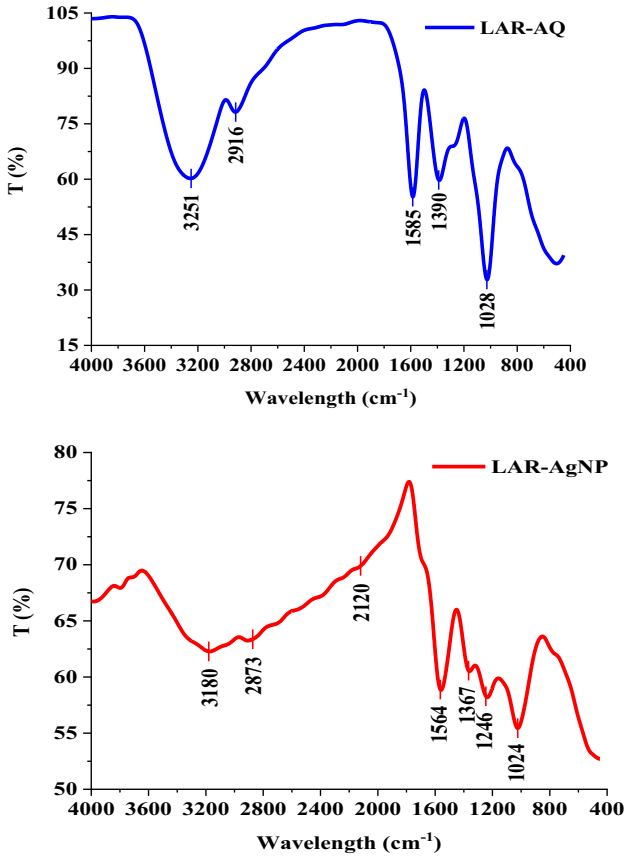


Fig. 4 FTIR spectrums for LAR-AQ and LAR-AgNP

are presented in Table 4. Thiourea for urease, acarbose for α-amylase, AChE, and BChE for galantamine served as a standard drug.

Increasing ammonia secretion and pH increase in urease metabolic activity dramatically helps in the proliferation of pathogenic *Helicobacter pylori*. The increase of this pathogen is the source of many diseases, such as urinary tract infections, intestinal infections, and gastrointestinal infections [61]. The LAR-AQ extract and LAR-AgNP completely inhibited the urease. The inhibition activity of AgNP was more effective than that of thiourea. AgNP's enzyme inhibition was significantly more effective than the aqueous root extract's, with a *p*-value of less than 0.05 (Table 4). LAR-AgNP can be preferred as an alternative product to control the pathogen *Helicobacter pylori*.

The inhibitory effects of root aqueous extract and AgNP on AChE and BChE activities were exhibited in Table 4. IC_{50} (µg/mL) values of LAR-AgNP (2.84 µg/mL) showed significantly higher BChE inhibitory effects compared to root aqueous extract (6.48 µg/mL). Moreover, the BChE inhibitory activity of galantamine (31.84 µg/mL) was lower than LAR-AgNP. AChE and BChE inhibitors are an important therapeutic strategy in the treatment of AD (Alzheimer's disease). In AD, high AChE and BChE activities are directly related to unexpected loss of cholinergic function and memory impairment. The result is the rapid hydrolysis of acetylcholine and butyrylcholine, which transmit nerve impulses from one neuron to another.

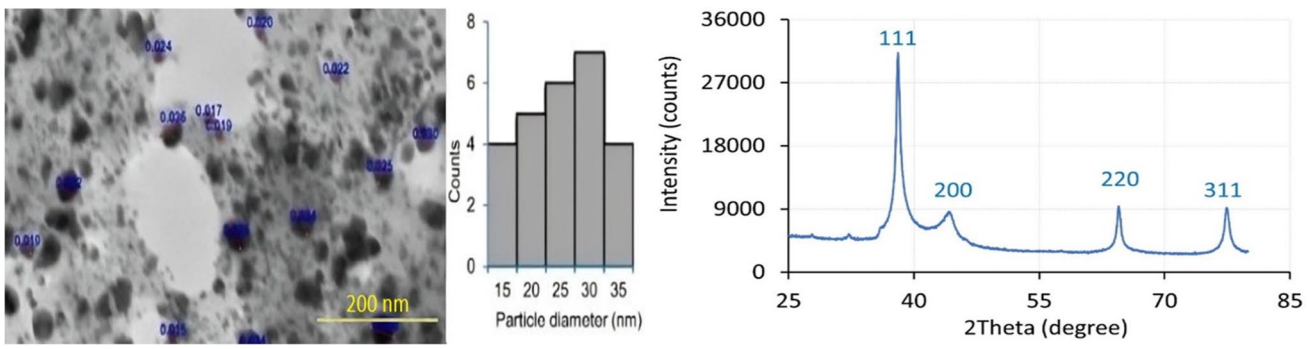


Fig. 5 TEM images and XRD pattern of synthesized LAR-AgNP

Therefore, the controlled availability of acetylcholine and butyrylcholine by inhibiting BChE enhances neuronal transmission and regulation of memory function. These observed inhibitory effects of water root extract on AChE and BChE may be beneficial in treating AD [62]. In particular, the best effects were obtained on the BChE activity of the extract and AgNP. Identification of new plant-derived BChE inhibitors will reveal target steps in the AD treatment strategy [63].

Table 4 displays the effects of acarbose and natural LAR-AQ extract on α-amylase inhibition. Inhibition of α-amylase was greater in LAR-AQ extract than in acarbose. Inhibition of α-amylase rose from LAR-AgNP to LAR-AQ to acarbose, as measured by their respective IC_{50} values. LAR-AgNP exhibited the strongest α-amylase inhibitory activity compared to the previous extracts, although it was not as effective in inhibiting α-amylase as the *Lactuca* species extracts seen here [64]. Compared to LAR-AQ extract, α-amylase inhibitor activity results previously reported by Zahra vb. [65] were lower. LAR-AQ may delay starch hydrolysis in the gastrointestinal tract, aiding in the management of diabetes on α-amylase activity. This process affects glucose absorption after meals, increasing and decreasing it.

3.4 Antimicrobial Activity

Recently, green synthesized AgNPs have increased their use in many areas, such as medicine, medical devices, testing, and food containers, due to their strong antimicrobial and antifungal potential against pathogenic and fungal microorganisms [66]. In this work, the antibacterial properties of LAR-AQ extract and LAR-AgNP with MIC and IZ values are displayed in Table 5 and compared with amoxicillin and tetracycline as positive control. When it came to *S. aureus* bacteria, the extracts were effective. It was discovered that the LAR-AgNP was effective against *B. cereus*, *P. aeruginosa*, *E. coli,* and *P. aeruginosa*. While a great deal of research has been done on the antibacterial properties of *L. anatolica*, variations in the chemical makeup of *Lactuca* species and alternative techniques for determining antibacterial activity make it challenging to compare the findings of various investigations [67–69]. Using the disc technique in this work, LAR-AgNP is the most efficient extract against the bacteria mentioned above, followed by tetracycline and amoxicillin.

Matching the results of different studies is difficult since various *Lactuca* species have different chemical compositions, and different methods are used to assess antibacterial activity. The antibacterial qualities of *Lactuca* types have been the subject of several studies, yet it might be difficult to compare the results of different researches. According to the latest research by Bensy, Christobel, Muthusamy, Alfarhan, and Anantharaman [15], Ishwarya, Vaseeharan, Kalyani, Banumathi, Govindarajan, Alharbi, Kadaikunnan, Al-Anbr, Khaled,

Table 3 Antioxidant activities of LAR-AQ and LAR-AgNP

Samples	PMRA	RPA	DPPH· scavenging	ABTS·+ scavenging	LPI
	Activity ($A_{0.5}$, μg/mL)		Activity (IC_{50}, μg/mL)		
LAR-AQ	7.06 ± 2.02^{a}	41.34 ± 0.13^{a}	1.86 ± 0.34^{a}	145.75 ± 1.45^{b}	16.28 ± 3.99^{c}
LAR-AgNP	0.10 ± 0.12^{a}	1.17 ± 0.01^{a}	2.61 ± 0.66^{a}	6.21 ± 3.37^{a}	1.10 ± 0.07^{a}
Ascorbic acid	1.38 ± 1.19^{a}	50.82 ± 0.00^{a}	2.33 ± 1.65^{a}	98.37 ± 0.47^{ab}	35.28 ± 0.20^{c}
Trolox	1.20 ± 0.17^{a}	30.37 ± 0.0^{a}	1.36 ± 0.26^{a}	6.51 ± 0.34^{a}	146.31 ± 2.44^{d}

Values are mean ± standard deviation; different superscript letters ($^{a–d}$) indicate significant differences in values within the same column ($p < 0.05$)

LAR-AQ L. anatolica root aqueous extract; *LAR-AgNP L. anatolica* root silver nanoparticles; *PMRA* phosphomolybdate reducing assay; *RPA* reducing power assay; *DPPH*· 2,2-diphenyl-1-picrylhydrazyl assay; *ABTS*·+ 2,2-azino-bis-3-ethylbenzothiazoline-6-sulfonic acid assay; *LPI* lipid peroxidation inhibition

Table 4 Enzyme inhibition potentials of LAR-AQ and LAR-AgNP

Samples	Urease	AChE	BChE	α-Amylase
	Activity (IC_{50}, μg/mL)			
LAR-AQ	7.94 ± 0.43^{a}	2.48 ± 1.12^{a}	6.48 ± 0.55^{a}	28.42 ± 3.29^{a}
LAR-AgNP	3.32 ± 0.47^{a}	32.49 ± 1.88^{a}	2.84 ± 1.14^{a}	4.93 ± 6.96^{a}
Standard drugs	6.03 ± 3.28^{a} (thiourea)	6.35 ± 2.96^{a} (galantamine)	31.84 ± 1.80^{a} (galantamine)	29.60 ± 4.97^{a} (acarbose)

LAR-AQ L. anatolica root aqueous extract; *LAR-AgNP L. anatolica* root silver nanoparticles; *AChE* Acetylcholinesterase; *BChE* Butyrylcholinesterase

Table 5 Antibacterial activities of LAR-AQ and LAR-AgNP

Sample/ Antibiotic	Gram-negative bacteria			Gram-positive bacteria		
	E. coli	*P. aeruginosa*	*K. pneumoniae*	*E. faecalis*	*S. aureus*	*B. cereus*
Inhibition zone (IZ, mm)						
LAR-AQ	9.0 ± 0.0	-	-	9.0 ± 0.0	-	8.5 ± 0.7
LAR-AgNP	10.5 ± 0.7	9.0 ± 0.0	9.0 ± 0.0	11.5 ± 0.7	10.5 ± 0.7	9.0 ± 0.0
Amoxicillin	15.5 ± 0.7	-	8.0 ± 0.0	-	26.5 ± 2.1	25.0 ± 0.0
Chloramphenicol	18.5 ± 0.7	18.0 ± 0.0	15.0 ± 0.0	13.5 ± 2.1	18.5 ± 0.7	25.0 ± 0.0
Minimum inhibitory concentrations (MIC, µg/mL)						
LAR-AQ	> 512	> 512	> 512	> 512	> 512	> 512
LAR-AgNP	256	128	256	256	256	256
Amoxicillin	16	> 1024	> 1024	> 1024	> 1024	> 1024
Tetracycline	8	> 512	> 512	> 512	128	512

LAR-AQ L. anatolica root aqueous extract; *LAR-AgNP L. anatolica* root silver nanoparticles

and Benelli [16], the MIC of both gram-positive and gram-negative bacteria agreed with our findings. Nonetheless, differences in phenolic compounds in the *Lactuca* nanoparticle extracts led to differences in inhibitory levels. *Lactuca* nanoparticle extract can be linked to the identified differences in inhibitory amounts.

3.5 Anti-inflammatory Effect

Protein denaturation has been linked to rheumatoid arthritis in many studies and is a well-known reason for inflammatory response. Protein denaturation in vivo may be responsible for autoantigen formation in various rheumatic diseases. Disulfide, hydrophobic, hydrogen, and electrostatic bonding changes are most likely part of the denaturation process. Various anti-inflammatory drugs have been shown to reduce heat-induced protein denaturation in a dose-dependent manner [70]. Therefore, phytochemicals from plants that can prevent denaturation of protein inhibition may be helpful in developing anti-inflammatory drugs [71]. Anti-inflammatory activities of LAR-AQ may have sprung from its capacity to inhibit heat-induced protein denaturation, as evidenced by the aqueous extract employed in this study. Standard diclofenac at 125 µg/mL inhibited the denaturation of BSA by 40.91%. In contrast, LAR-AQ and LAR-AgNP in vitro anti-inflammation efficacy by BSA denaturation method revealed 65.15 and 57.58% inhibition, respectively (Fig. 6). This study was able to demonstrate the effects of LAR-AQ extract and optimized LAR-AgNP on preventing, controlling, and inhibiting BSA denaturation, and its effect was comparable to standard diclofenac. These results are similar to the in vitro anti-inflammatory results tested on aqueous extracts of *Lactuca* species [68, 72, 73].

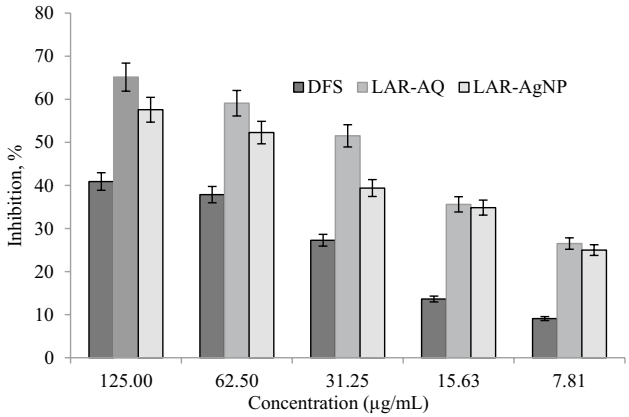
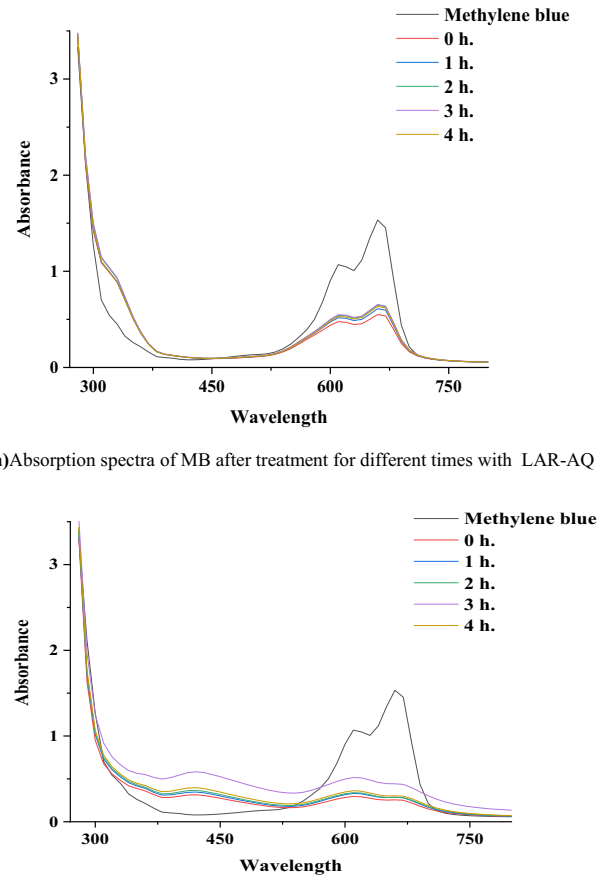


Fig. 6 Inhibition of BSA protein denaturation potential of LAR-AgNP and LAR-AQ

3.6 Photocatalytic Activity

The photocatalytic reduction of MB dye was examined utilizing biosynthesized LAR-AgNP utilized at various time points. Figure 7 depicts the photodegradation of MB under visible light irradiation in the absence of a catalyst and in the presence of produced LAR-AgNP and bulk LAR-AQ extract. The typical absorption peak of the MB solution was 663 nm. The MB concentration remained relatively constant without a photocatalyst in the blank test. In contrast, once the catalyst was introduced to the mixture, the quantity of MB was significantly reduced. The produced LAR-AgNP was shown to be more active in photodegrading MB than the LAR-AQ extract. MB degradation was observed as a decrease in peak intensity after 5 h of incubation. Without Ag nanocatalysts, there is no appreciable shift in the peak position of MB. When a metal catalyst is present, visible light decolorizes methyl blue faster than other irradiation methods. The adsorption of Ag nanoparticles onto the



a)Absorption spectra of MB after treatment for different times with LAR-AQ

b)Absorption spectra of MB after treatment for different times with LAR-AgNP

Fig. 7 UV-vis spectrums of LAR-AQ extract (**a**) and synthesized LAR-AgNP (**b**) at different times for photocatalytic activity

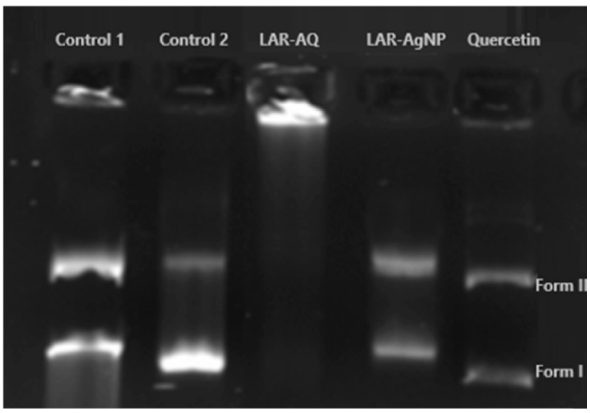
MB solution began slowly and then increased with time. Overall, Ag nanoparticles' photocatalytic activities in visible light may be attributed to the stimulation of surface plasmon resonance (SPR), a charge density oscillation that may propagate at the interface between metal and dielectric medium; Kumar et al. [74] and Wang et al. [75] state this.

3.7 DNA Protection Activity

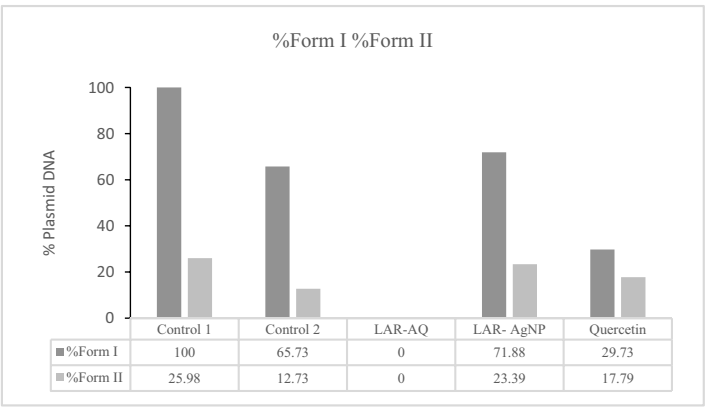
The effectiveness of LAR-AQ extract, LAR-AgNP, and quercetin, which act as a reference, in protecting DNA was assessed using agarose gel electrophoresis (Fig. 8). Compared to the form I structure of LAR-AgNP, the control 2 and the quercetin standard are darker. The same holds true for the form II structure. It was found that LAR-AgNP shielded 71.88% of the DNA's form I structure. The activity of LAR-AgNP shields DNA. Form I and form II values in Fig. 8 illustrate how the samples affected the plasmid DNA structure. Because of these qualities, biosynthesized AgNP exhibited more potential DNA protection activity than quercetin.

3.8 Proposed Mechanism of Biosynthesized AgNP

The green synthesis of AgNPs was produced by the interaction of LAR-AQ extract with $AgNO_3$ solution. AgNP development is indicated by the change from yellow to dark brown [76]. Thus, in the HPLC–MS/MS analysis of the aqueous root extract of LAR-AQ extract, it was seen that the presence of phenolic compounds was responsible for the bioreduction of Ag^+ into AgNPs. It has been suggested that the mechanism of nanoparticle formation affects the main compound, chlorogenic acid (Fig. 9). The LAR-AQ extract included secondary metabolites that reduced, encapsulated, and stabilized Ag ions. Chlorogenic acid was utilized for the reaction process as quantitative research showed that it was an essential part of the root extract.



(a) Agarose gel electrophoresis image



(b) Percentage distribution of Form I and Form II plasmid DNA

Fig. 8 DNA protection activities of LAR-AQ and synthesized LAR-AgNP (**a/ b**)

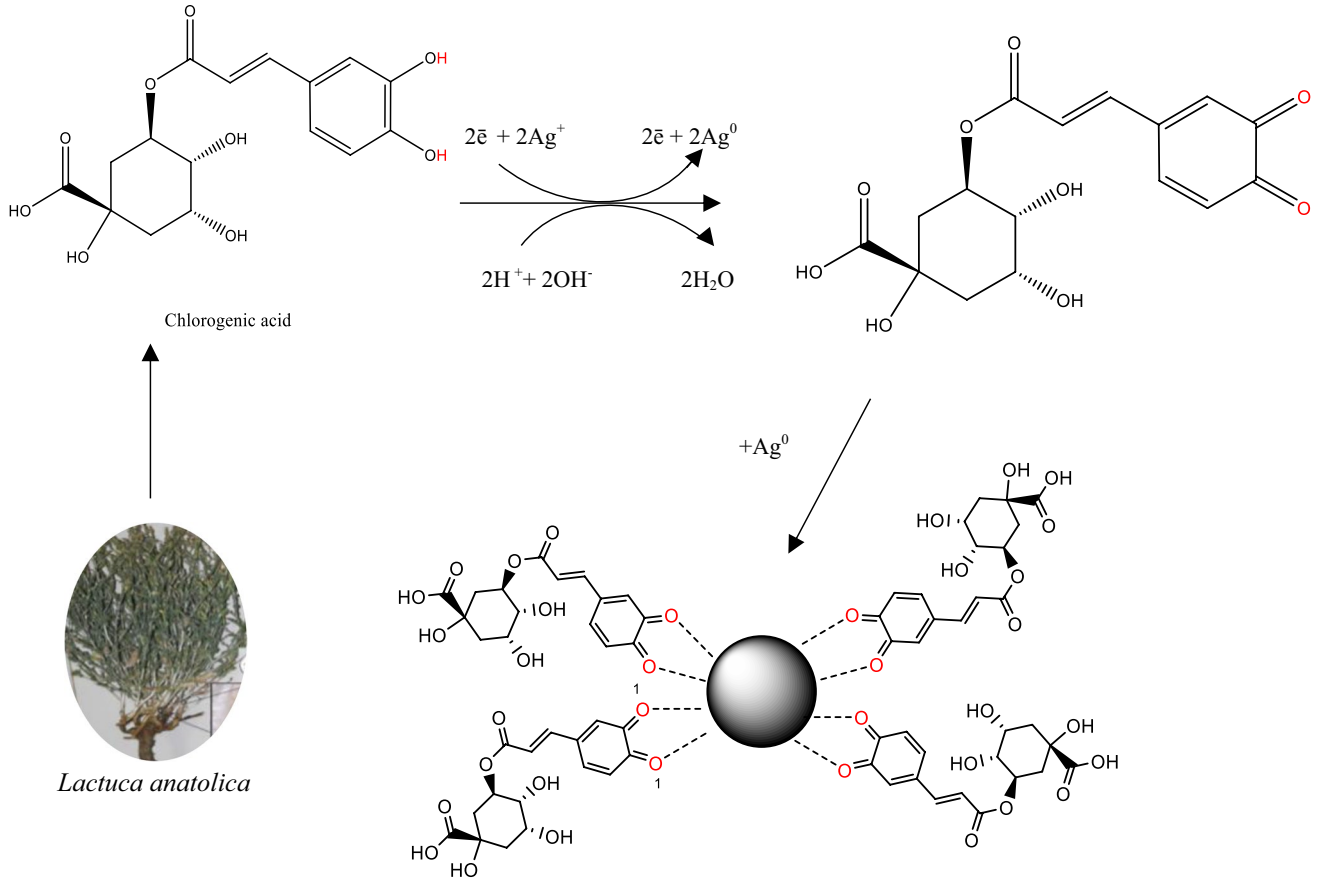


Fig. 9 The reaction mechanism of silver nanoparticle production (chlorogenic acid-AgNP)

3.9 Molecular Docking

The results of the nanoparticles were high in general and attracted attention, especially against bacteria. Compared to the aqueous extracts, the our nanoparticles showed high effect, also were active even against the bacteria strains that the aqueous extract showed no activity on them. Therefore, to clarify the extent of the effect, we studied molecular docking to understand the mechanism of the effect of these compounds, in their hypothetical structure with the highest probability, on the common antibiotic targets between the bacteria strains used in this work. The first target was DD-transpeptidase, with a MolDock score of − 203 for the interaction. Here, the molecular docking results revealed the formation of a total of 17 interactions between the chlorogenic acid-AgNP and the protein, as follows: 11 conventional hydrogen bonds between the protein and SER62, ASN117, THR123, ARG287, SER290, PHE120, ARG287, THR123, and ASP288 and 2 bonds with ASP114 residue; three carbon-hydrogen bonds with ARG337, THR123, and ASN333 residues; and three Pi-alkyl hydrophobic interactions with LEU332, ALA336, and LEU332 residues (Fig. 10).

Dihydrofolate reductase gave a total of 15 interactions with the nanoparticle molecule with an interaction MolDock score − 238: six conventional hydrogen bonds with ASN5, GLU82, GLU107, ASN124, ARG191, and ASN123 residues; six carbon-hydrogen bonds with ARG108, SER95, and ASN119 and three with GLU120 residue; Pi-Pi T-shaped hydrophobic interaction with HIS129, one Alkyl hydrophobic interaction with LYS45, and one Pi-alkyl hydrophobic interaction with ILE96 residue (Fig. 11).

The last antibiotic target was gyrase, the docking results for this protein with the nanoparticles and gave an interaction MolDock score − 238 and a total of 15 interactions as follows: six conventional hydrogen bonds with ASN1149, GLU1156, ASP1148, ALA509, GLY1082, and LYS460 residues; two carbon hydrogen bonds with GLY436 and HIS1081 residues; one Pi-anion hydrophobic interaction with ASP512 residue, Pi-donor hydrogen bond with ARG1122 residue, Pi-Pi stacked hydrophobic interaction with HIS1081 residue, and four more Pi-Alkyl hydrophobic interactions divided between LYS581 and PRO1080 residues (Fig. 12).

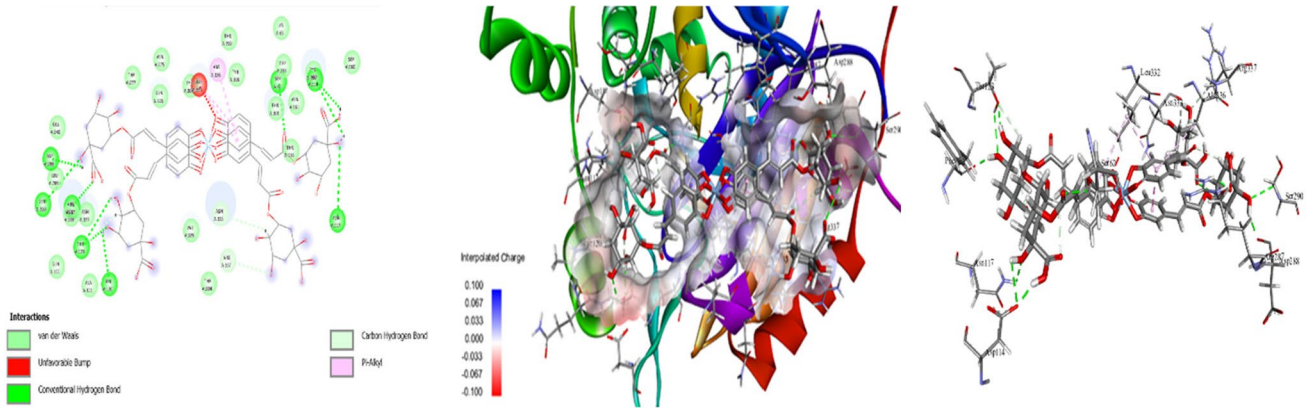


Fig. 10 Molecular docking between the DD-transpeptidase and nanoparticale (chlorogenic acid-AgNP)

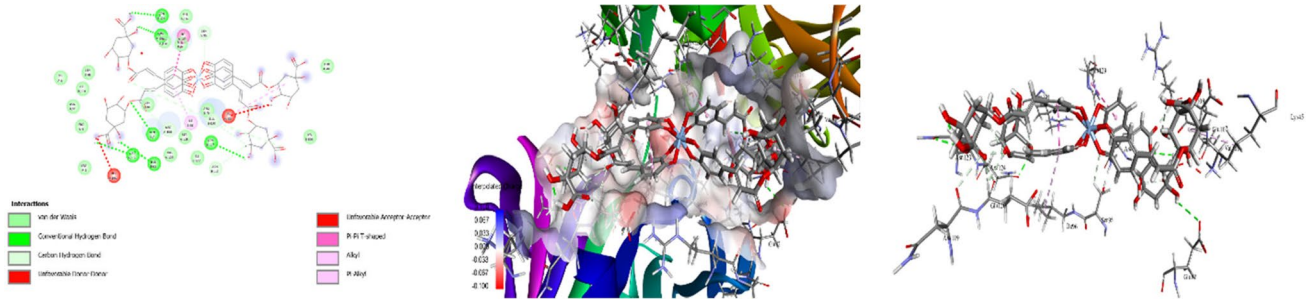


Fig. 11 Molecular docking between the dihydrofolate reductase and nanoparticale (chlorogenic acid-AgNP)

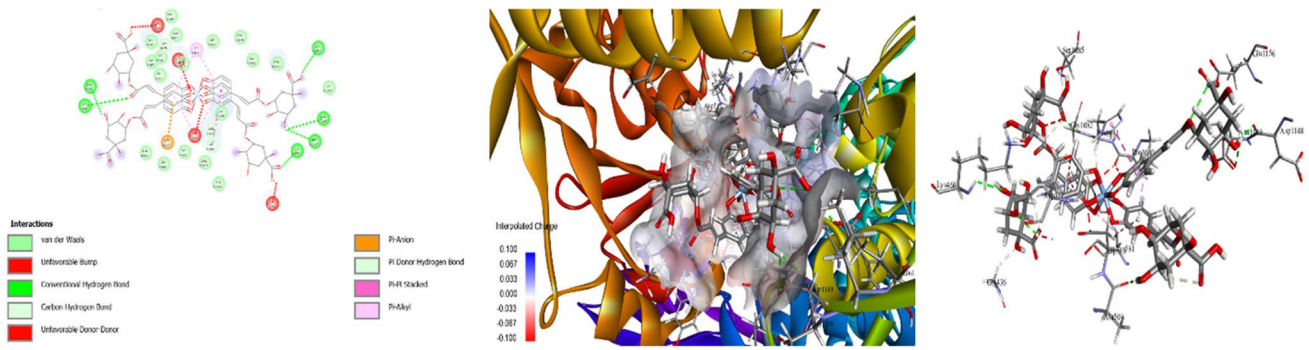


Fig. 12 Molecular docking between the gyrase and nanoparticale (chlorogenic acid-AgNP)

The application of computational modeling may yield unique insights into the workings of the antimicrobial compounds' methods of action, hence impeding the development of infection. The compounds that might bind selectively to the protein's active regions that cause infections by bacteria were predicted using the molecular docking technique [77, 78]. In other studies, it has been found that nanoparticles have a promising binding interactions especially among the hydroxyl groups against different antibacterial targets; as in our study, we observed high binding affinity of our model particle with both DNA gyrase and dihydrofolate reductase, due to the many hydrogen bonds between the hydroxyl grubs and proteins [79].

4 Conclusion

This investigation examined the capabilities of LA-AgNPs, which were ground up and synthesized using distilled water. The results demonstrated the interplay between a

high metabolite concentration and various phenolic characteristics that function. The LAR-AgNP extract included many bioactive compounds with strong urease, AChE, BChE, and α-amylase inhibitory activities and enhanced $ABTS^{\bullet+}$ scavenging and LPI activity. The LAR-AgNP extract showed a strong ability to scavenge $DPPH^{\bullet}$ and an impressive inhibitory activity against gram-positive bacteria and gram-negative bacteria. The high phenol content of the *L. anatolica* extract reduced the damage to DNA caused by H_2O_2 and UV radiation. Our research validates *L. anatolica*'s perspective as a beneficial source of antioxidation, antibacterial medication, inhibiting enzyme, and DNA protector. It is used as a restorative material and natural dietary supplement for regulating human health. In addition, we obtained impressive results from molecular docking of the expected structure of *L. anatolica*'s aqueous extract nanoparticles against many antibiotic targets. This, in turn, explains the remarkable antibacterial scores of the in vitro test. This study shows that *L. anatolica* extract includes a range of bioactive phenolic compounds with substantial biological activity. For a cheap cost, a high extraction rate of *L. anatolica* extract may be achieved economically. From a medicinal perspective, extracts of *L. anatolica* are safe and easy to digest. The high and promising biological effectiveness of the nanoparticle compounds as well as the extracts indicates the striking results that can be obtained in future in vivo tests. Moreover, due to the abundance of this species in nature and the varied medical advantages of *L. anatolica*, it will definitely lead researchers 1 day to use this species as a source for medical drugs.

Acknowledgements It should not be shared with third parties during the manuscript evaluation process or in case the evaluation results negatively. If the evaluation is positive, rights are reserved with BioNanoScience.

We accept the following statement at the "BioNanoScience" evaluation stage of the study.

*Authors can also choose to publish under the traditional publishing model (no APC charges apply); both options will be offered after the paper has been accepted.

We would like to thank Ondokuz Mayıs University and Scientific Research Projects Coordination Unit for supporting the research project (PYO.FEN.1904.22.024) of this master's thesis.

Author Contribution Ramazan Erenler and Ilyas Yıldız performed the plant extraction and synthesis of AgNPs. Bioactivities and manuscript preparation were performed by Noor Hassan Nayel Nayel, Sarmad Marah, the collection of plants was carried out by Lutfi Behcet, and manuscript preparation and project design were carried out by Tevfik Ozen.

Data Availability No datasets were generated or analysed during the current study.

Declarations

Informed Consent Informed consent rules were not applicable to this research because no human participants were involved.

Competing interests The authors declare no competing interests.

Research Involving Human Participants and/or Animals None.

References

1. Ahmad, N., Ali, S., Abbas, M., Fazal, H., Saqib, S., Ali, A., Ullah, Z., Zaman, S., Sawati, L., & Zada, A. (2023). Antimicrobial efficacy of Mentha piperata-derived biogenic zinc oxide nanoparticles against UTI-resistant pathogens. *Scientific Reports., 13*, 14972.
2. Sharif, M. S., Hameed, H., Waheed, A., Tariq, M., Afreen, A., Kamal, A., Mahmoud, E. A., Elansary, H. O., Saqib, S., & Zaman, W. (2023). Biofabrication of Fe3O4 nanoparticles from spirogyra hyalina and ajuga bracteosa and their antibacterial applications. *Molecules, 28*, 3403.
3. Ravindran, A., Chandran, P., & Khan, S. S. (2013). Biofunctionalized silver nanoparticles: Advances and prospects. *Colloids and Surfaces B: Biointerfaces., 105*, 342–352.
4. Yu, S. J., Yin, Y. G., & Liu, J. F. (2013). Silver nanoparticles in the environment. *Environmental Science: Processes & Impacts., 15*, 78–92.
5. Saqib, S., Nazeer, A., Ali, M., Zaman, W., Younas, M., Shahzad, A., & Sunera, and M. Nisar,. (2022). Catalytic potential of endophytes facilitates synthesis of biometallic zinc oxide nanoparticles for agricultural application. *BioMetals., 35*, 967–985.
6. Saqib, S., Faryad, S., Afridi, M. I., Arshad, B., Younas, M., Naeem, M., Zaman, W., Ullah, F., Nisar, M., & Ali, S. (2022). Bimetallic assembled silver nanoparticles impregnated in Aspergillus fumigatus extract damage the bacterial membrane surface and release cellular contents. *Coatings, 12*, 1505.
7. Iravani, S., Korbekandi, H., Mirmohammadi, S. V., & Zolfaghari, B. (2014). Synthesis of silver nanoparticles: Chemical, physical and biological methods. *Research in pharmaceutical sciences., 9*, 385.
8. Reaka-Kudla, M. L., Wilson, D. E., & Wilson, E. O. (1996). *Biodiversity II: understanding and protecting our biological resources*. Joseph Henry Press.
9. Bohm, B. A., & Stuessy, T. F. (2001). *Flavonoids of the sunflower family (Asteraceae)*. Springer Science & Business Media.
10. Manzoor, M., Ahmad, M., Zafar, M., Gillani, S. W., Shaheen, H., Pieroni, A., Al-Ghamdi, A. A., Elshikh, M. S., Saqib, S., & Makhkamov, T. (2023). The local medicinal plant knowledge in Kashmir Western Himalaya: A way to foster ecological transition via community-centred health seeking strategies. *Journal of Ethnobiology and Ethnomedicine., 19*, 56.
11. Ullah, F., Saqib, S., Khan, W., Ayaz, A., Batool, A., Wang, W.-Y., & Xiong, Y.-C. (2024). The multifaceted role of sodium nitroprusside in plants: Crosstalk with phytohormones under normal and stressful conditions. *Plant Growth Regulation*. 1–18
12. Staneva, J. D., Todorova, M. N., & Evstatieva, L. N. (2008). Sesquiterpene lactones as chemotaxonomic markers in genus Anthemis. *Phytochemistry, 69*, 607–618.
13. Zidorn, C. (2008). Sesquiterpene lactones and their precursors as chemosystematic markers in the tribe Cichorieae of the Asteraceae. *Phytochemistry, 69*, 2270–2296.
14. Achika, J. I., Arthur, D. E., Gerald, I., & Adedayo, A. (2014). A review on the phytoconstituents and related medicinal properties of plants in the Asteraceae family. *IOSR Journal of Applied Chemistry, 7*, 1–8.
15. Bensy, A. D., Christobel, G. J., Muthusamy, K., Alfarhan, A., & Anantharaman, P. (2022). Green synthesis of iron nanoparticles from Ulva lactuca and bactericidal activity against enteropathogens. *Journal of King Saud University-Science., 34*, 101888.

16. Ishwarya, R., Vaseeharan, B., Kalyani, S., Banumathi, B., Govindarajan, M., Alharbi, N. S., Kadaikunnan, S., Al-Anbr, M. N., Khaled, J. M., & Benelli, G. (2018). Facile green synthesis of zinc oxide nanoparticles using Ulva lactuca seaweed extract and evaluation of their photocatalytic, antibiofilm and insecticidal activity. *Journal of Photochemistry and Photobiology B: Biology., 178*, 249–258.
17. Zahra, Z., Arshad, M., Rafique, R., Mahmood, A., Habib, A., Qazi, I. A., & Khan, S. A. (2015). Metallic nanoparticle (TiO2 and Fe3O4) application modifies rhizosphere phosphorus availability and uptake by Lactuca sativa. *Journal of agricultural and food chemistry., 63*, 6876–6882.
18. Devi, J. & Bhimba, B. (2012). Anticancer activity of silver nanoparticles synthesized by the seaweed *Ulva lactuca* in vitro, *Scientific Reports, 1*(242), 2–5.
19. Shobier, A., & El Ashry, E. (2021). Pharmacological applications of the green seaweed Ulva lactuca. *Russian Journal of Marine Biology., 47*, 425–439.
20. Behçet, L., & Yapar, Y. (2020). Lactuca anatolica (Asteraceae: Lactucinae), a new species from eastern Anatolia (Turkey). *Phytotaxa., 455*, 287–294.
21. Erenler, R., Geçer, E. N., Nusret, G., & Yanar, D., (2021). Antioxidant activity of silver nanoparticles synthesized from Tagetes erecta L. leaves. *International Journal of Chemistry and Technology., 5*, 141–146.
22. Karan, T., Erenler, R., Gonulalan, Z., & Kolemen, U. (2023). Biogenic synthesis of silver nanoparticles using Sambucus nigra leaves: elucidation, antimicrobial, antioxidant activities and quantification of phenolics. *Chemical Papers*, 1–9.
23. Singleton, V. L., & Rossi, J. A. (1965). Colorimetry of total phenolics with phosphomolybdic-phosphotungstic acid reagents. *American journal of Enology and Viticulture., 16*, 144–158.
24. C.-C. Chang, M.-H. Yang, H.-M. Wen, and J.-C. Chern, Estimation of total flavonoid content in propolis by two complementary colorimetric methods. *Journal of food and drug analysis*. 10, (2002)
25. Ozen, T., Bora, N., Yenigun, S., & Korkmaz, H. (2020). An investigation of chemical content, enzyme inhibitory propert, antioxidant and antibacterial activity of *Aristolochia bodamae* Dingler (develiotu)(Aristolochiaceae) root extracts from Samsun. *Turkey. Flavour and Fragrance Journal., 35*, 270–283.
26. Prieto, P., Pineda, M., & Aguilar, M. (1999). Spectrophotometric quantitation of antioxidant capacity through the formation of a phosphomolybdenum complex: Specific application to the determination of vitamin E. *Analytical Biochemistry., 269*, 337–341.
27. Oyaizu, M. (1986). Studies on products of browning reaction antioxidative activities of products of browning reaction prepared from glucosamine. *The Japanese journal of nutrition and dietetics., 44*, 307–315.
28. Blois, M. S. (1958). Antioxidant determinations by the use of a stable free radical. *Nature, 181*, 1199–1200.
29. Re, R., Pellegrini, N., Proteggente, A., Pannala, A., Yang, M., & Rice-Evans, C. (1999). Antioxidant activity applying an improved ABTS radical cation decolorization assay. *Free radical biology and medicine., 26*, 1231–1237.
30. Dinis, T. C., Madeira, V. M., & Almeida, L. M. (1994). Action of phenolic derivatives (acetaminophen, salicylate, and 5-aminosalicylate) as inhibitors of membrane lipid peroxidation and as peroxyl radical scavengers. *Archives of Biochemistry and Biophysics., 315*, 161–169.
31. Bibi Sadeer, N., Sinan, K. I., Cziáky, Z., Jekő, J., Zengin, G., Jeewon, R., Jeewon, R., Abdallah, H. H., AlDhaheri, Y. A., Eid,H., & Mahomoodally, M. F. (2022). Towards the pharmacological validation and phytochemical profiling of the decoction and maceration of Bruguiera gymnorhiza (L.) lam.—a traditionally used medicinal halophyte. *Molecules, 27(6)*, 2000.
32. Zhang, L., Mulrooney, S. B., Leung, A. F., Zeng, Y., Ko, B. B., Hausinger, R. P., & Sun, H. (2006). Inhibition of urease by bismuth (III): Implications for the mechanism of action of bismuth drugs. *BioMetals, 19*, 503–511.
33. Ellman, G. L., Courtney, K. D., Andres, V., Jr., & Featherstone, R. M. (1961). A new and rapid colorimetric determination of acetylcholinesterase activity. *Biochemical Pharmacology., 7*, 88–95.
34. Özçelik, A. B., Gökçe, M., Orhan, I., & Sahin, M. F. (2010). Synthesis and acetylcholinesterase/butyrylcholinesterase inhibitory activities of (substituted/nonsubstituted benzal) hydrazone derivatives of 3-(6-substituted-3 (2H)-pyridazinon-2-yl) propionohydrazides/3-(6-Sübstitüe-3 (2H)-piridazinon-2-il) Propiyionohidrazit Türevlerinin (Sübstitüe/Nonsübsitüe Benzal) Hidrazon bilesiklerinin Sentezi ve Asetilkolinesteraz/Butirilkolinesteraz Inhibitörü Aktivitesi. *FABAD Journal of Pharmaceutical Sciences., 35*, 153.
35. Andrews, J. M. (2001). Determination of minimum inhibitory concentrations. *Journal of Antimicrobial Chemotherapy., 48*, 5–16.
36. Reller, L. B., Weinstein, M., Jorgensen, J. H., & Ferraro, M. J. (2009). Antimicrobial susceptibility testing: A review of general principles and contemporary practices. *Clinical Infectious Diseases., 49*, 1749–1755.
37. Rahman, H., Eswaraiah, M. C., Vakati, K., & Madhavi, P. (2012). In vitro studies suggest probable mechanism of eucalyptus oil for anti-inflammatory and anti-arthritic activity. *International Journal of Phytopharmacy, 2*, 81–83.
38. Miri, A., Shahraki Vahed, H. O., & Sarani, M. (2018). Biosynthesis of silver nanoparticles and their role in photocatalytic degradation of methylene blue dye. *Research on Chemical Intermediates., 44*, 6907–6915.
39. Y. Başar, S. Yenigün, Y. İpek, L. Behçet, F. Gül, T. Özen, and İ. Demirtaş (2023) DNA protection, molecular docking, enzyme inhibition and enzyme kinetic studies of 1, 5, 9-epideoxyloganic acid isolated from Nepeta aristata with bio-guided fractionation. *Journal of Biomolecular Structure and Dynamics*. 1–14
40. Berman, H. M., Westbrook, J., Feng, Z., Gilliland, G., Bhat, T. N., Weissig, H., Shindyalov, I. N., & Bourne, P. E. (2000). The protein data bank. *Nucleic acids research., 28*, 235–242.
41. Alyar, S., Özmen, Ü. Ö., Adem, Ş, Alyar, H., Bilen, E., & Kaya, K. (2021). Synthesis, spectroscopic characterizations, carbonic anhydrase II inhibitory activity, anticancer activity and docking studies of new Schiff bases of sulfa drugs. *Journal of Molecular Structure., 1223*, 128911.
42. Thomsen, R., & Christensen, M. H. (2006). MolDock: A new technique for high-accuracy molecular docking. *Journal of Medicinal Chemistry., 49*, 3315–3321.
43. Biovia, D. S. (2019). Biovia discovery studio visualize 2019, version 2019. *Dassault Systèmes Biovia:* San Diego, CA, USA.
44. Yenigun, S., Ipek, Y., Marah, S., Demirtas, I., & Ozen, T. (2024). DNA protection, molecular docking, antioxidant, antibacterial, enzyme inhibition, and enzyme kinetic studies for parietin, isolated from Xanthoria parietina (L.) Th. *Fr. Journal of Biomolecular Structure and Dynamics., 42*, 848–862.
45. Pammi, S. S., Suresh, B., & Giri, A. (2023). Antioxidant potential of medicinal plants. *Journal of Crop Science and Biotechnology., 26*, 13–26.
46. Nwozo, O. S., Effiong, E. M., Aja, P. M., & Awuchi, C. G. (2023). Antioxidant, phytochemical, and therapeutic properties of medicinal plants: A review. *International Journal of Food Properties., 26*, 359–388.
47. Stanciu, G., Aonofriesei, F., Lupsor, S., Oancea, E., & Mititelu, M. (2023). Chemical composition, antioxidant activity, and

antibacterial activity of black poplar buds' hydroalcoholic macerates from dobrogea area. *Molecules, 28*, 4920.
48. Harsha, S., Anilakumar, K., & Mithila, M. (2013). Antioxidant properties of Lactuca sativa leaf extract involved in the protection of biomolecules. *Biomedicine & Preventive Nutrition., 3*, 367–373.
49. Stojakowska, A., & Malarz, J. (2017). Bioactive phenolics from in vitro cultures of Lactuca aculeata Boiss. et Kotschy. *Phytochemistry Letters., 19*, 7–11.
50. Gan, Y., & Azrina, A. (2016). Antioxidant properties of selected varieties of lettuce (*Lactuca sativa* L.) commercially available in Malaysia. *International Food Research Journal*, *23*(6), 2357–2362.
51. Karan, T., Gonulalan, Z., Erenler, R., Kolemen, U., & Eminagaoglu, O. (2024). Green synthesis of silver nanoparticles using Sambucus ebulus leaves extract: Characterization, quantitative analysis of bioactive molecules, antioxidant and antibacterial activities. *Journal of Molecular Structure., 1296*, 136836.
52. Nazeer, A., Ahmad, F., Verma, N., & Ahmad, S., (2023). Targeted delivery of nanopesticides and nanofertilizers in sustainable agricultural farming. Cham: Springer Nature Switzerland, 125–139.
53. Karan,Y. B., & Erenler, R., (2024). Synthesis of silver nanoparticles using potato cultivars with their antioxidant activity. *Communications in Soil Science and Plant Analysis*, 1–9.
54. Daoudi, H., Bouafia, A., Meneceur, S., Laouini, S. E., Belkhalfa, H., Lebbihi, R., & Selmi, B. (2022). Secondary metabolite from nigella sativa seeds mediated synthesis of silver oxide nanoparticles for efficient antioxidant and antibacterial activity. *Journal of Inorganic and Organometallic Polymers and Materials., 32*, 4223–4236.
55. Hamouda, R. A., Alharthi, M. A., Alotaibi, A. S., Alenzi, A. M., Albalawi, D. A., & Makharita, R. R. (2023). Biogenic nanoparticles silver and copper and their composites derived from marine Alga Ulva lactuca: Insight into the characterizations, antibacterial activity, and anti-biofilm formation. *Molecules, 28*, 6324.
56. Sondi, I., & Salopek-Sondi, B. (2004). Silver nanoparticles as antimicrobial agent: a case study on E. coli as a model for gram-negative bacteria. *Journal of colloid and interface science., 275*, 177–182.
57. Fetyan, N. A., Essa, T. A., Salem, T. M., Taha, A. A., Elgobashy, S. F., Tharwat, N. A., & Elsakhawy, T. (2024). Promising eco-friendly nanoparticles for managing bottom rot disease in lettuce (Lactuca sativa var. Longifolia). *Microbiology Research., 15*, 196–212.
58. Sambhy, V., MacBride, M. M., Peterson, B. R., & Sen, A. (2006). Silver bromide nanoparticle/polymer composites: Dual action tunable antimicrobial materials. *Journal of the American Chemical Society., 128*, 9798–9808.
59. Amin, H. H. (2020). Biosynthesized silver nanoparticles using Ulva lactuca as a safe synthetic pesticide (in vitro). *Open Agriculture., 5*, 291–299.
60. González-Ballesteros, N., Rodríguez-Argüelles, M. C., Prado-López, S., Lastra, M., Grimaldi, M., Cavazza, A., Nasi, L., Salviati, G., & Bigi, F. (2019). Macroalgae to nanoparticles: study of Ulva lactuca L. role in biosynthesis of gold and silver nanoparticles and of their cytotoxicity on colon cancer cell lines. *Materials Science and Engineering: C., 97*, 498–509.
61. Bhattacharjee, A., Sahoo, O. S., Sarkar, A., Bhattacharya, S., Chowdhury, R., Kar, S., & Mukherjee, O. (2024). Infiltration to infection: Key virulence players of Helicobacter pylori pathogenicity. *Infection*, 1–40
62. Erdogan Orhan, I. (2012). Current concepts on selected plant secondary metabolites with promising inhibitory effects against enzymes linked to Alzheimer's disease. *Current Medicinal Chemistry., 19*, 2252–2261.
63. Darvesh, S. (2016). Butyrylcholinesterase as a diagnostic and therapeutic target for Alzheimer's disease. *Current Alzheimer Research., 13*, 1173–1177.
64. Vongsak, B., Kongkiatpaiboon, S., Jaisamut, S., Machana, S., & Pattarapanich, C. (2015). In vitro alpha glucosidase inhibition and free-radical scavenging activity of propolis from Thai stingless bees in mangosteen orchard. *Revista Brasileira de Farmacognosia., 25*, 445–450.
65. Zahra, S. A., Iqbal, J., Abbasi, B. A., Shahbaz, A., Kanwal, S., Shah, S. L., Ahmad, P., & Mahmood, T. (2021). Antimicrobial, cytotoxic, antioxidants, enzyme inhibition activities, and scanning electron microscopy of Lactuca orientalis (Boiss.) Boiss. seeds. *Microscopy Research and Technique., 84*, 1284–1295.
66. Aguda, O., & Lateef, A. (2022). Recent advances in functionalization of nanotextiles: a strategy to combat harmful microorganisms and emerging pathogens in the 21st century. *Heliyon, 8*(6), e09761.
67. Ibrahim, M. I., Amer, M. S., Ibrahim, H. A., & Zaghloul, E. H. (2022). Considerable production of ulvan from Ulva lactuca with special emphasis on its antimicrobial and anti-fouling properties. *Applied Biochemistry and Biotechnology., 194*, 3097–3118.
68. Pepe, G., Sommella, E., Manfra, M., De Nisco, M., Tenore, G. C., Scopa, A., Sofo, A., Marzocco, S., Adesso, S., & Novellino, T. (2015). Evaluation of anti-inflammatory activity and fast UHPLC–DAD–IT-TOF profiling of polyphenolic compounds extracted from green lettuce (Lactuca sativa L.; var. Maravilla de Verano). *Food Chemistry., 167*, 153–161.
69. Garayemi, S., & Raeisi, F. (2020). Graphene oxide as a docking station for modern drug delivery system. by Ulva lactuca species study its antimicrobial, anti-fungal and anti-blood cancer activity. *Advances in Applied NanoBio-Technologies., 1*, 53–62.
70. Rahman, H., Eswaraiah, M. C., & Dutta, A. (2015). In-vitro anti-inflammatory and anti-arthritic activity of Oryza Sativa Var. joha rice (an aromatic indigenous rice of Assam). *Am Eurasian J Agric Environ Sci, 15*, 115–121.
71. Gunathilake, K., Ranaweera, K., & Rupasinghe, H. V. (2018). In vitro anti-inflammatory properties of selected green leafy vegetables. *Biomedicines., 6*, 107.
72. Ololade, Z., Kuyooro, S., Ogunmola, O., & Abiona, O. (2017). Phytochemical, antioxidant, anti-arthritic, anti-inflammatory and bactericidal potentials of the leaf extract of Lactuca teraxacifolia. *Global Journal of Medical Research., 17*, 19–28.
73. Tong, T., Liu, Y.-J., Zhang, P., & Kang, S.-G. (2020). Antioxidant, anti-inflammatory, and α-amylase inhibitory activities of Ulva lactuca extract. *Korean Journal of Food Preservation., 27*, 513–521.
74. Kumar, P., Govindaraju, M., Senthamilselvi, S., & Premkumar, K. (2013). Photocatalytic degradation of methyl orange dye using silver (Ag) nanoparticles synthesized from Ulva lactuca. *Colloids and Surfaces B: Biointerfaces, 103*, 658–661.
75. Wang, P., Huang, B., Zhang, X., Qin, X., Dai, Y., Jin, H., Wei, J., & Whangbo M. H. (2008). Composite semiconductor H2WO4·H2O/AgCl as an efficient and stable photocatalyst under visible light. *Chemistry–A European Journal, 14*, 10543–10546
76. Kaviya, S., Santhanalakshmi, J., Viswanathan, B., Muthumary, J., & Srinivasan, K. (2011). Biosynthesis of silver nanoparticles using Citrus sinensis peel extract and its antibacterial activity. *Spectrochimica Acta Part A: Molecular and Biomolecular Spectroscopy., 79*, 594–598.
77. Toubi, Y., Abrigach, F., Radi, S., Souna, F., Hakkou, A., Alsayari, A., Bin Muhsinah, A., & Mabkhot, Y. N. (2019). Synthesis, antimicrobial screening, homology modeling, and molecular docking studies of a new series of Schiff base derivatives as prospective fungal inhibitor candidates. *Molecules., 24*, 3250.

78. Omar, H. S., Abd El-Rahman, S. N., AlGhannam, S. M., Reyad, N.E.-H.A., & Sedeek, M. S. (2021). Antifungal evaluation and molecular docking studies of Olea europaea leaf extract, Thymus vulgaris and Boswellia carteri essential oil as prospective fungal inhibitor candidates. *Molecules., 26*, 6118.
79. Nallappan, D., Fauzi, A. N., Krishna, B. S., Kumar, B. P., Reddy, A. V. K., Syed, T., Reddy, C. S., Yaacob, N. S., & Rao, P. V. (2021). Green biosynthesis, antioxidant, antibacterial, and anti-cancer activities of silver nanoparticles of Luffa acutangula leaf extract. *BioMed research international., 2021*, 1–28.

Publisher's Note Springer Nature remains neutral with regard to jurisdictional claims in published maps and institutional affiliations.

Springer Nature or its licensor (e.g. a society or other partner) holds exclusive rights to this article under a publishing agreement with the author(s) or other rightsholder(s); author self-archiving of the accepted manuscript version of this article is solely governed by the terms of such publishing agreement and applicable law.